

CHANDRA OBSERVATIONS OF THE GAMMA-RAY BINARY LS I +61 303: EXTENDED X-RAY STRUCTURE?

JOSEP M. PAREDES,¹ MARC RIBÓ,¹ VALENTÍ BOSCH-RAMON,² JENNIFER R. WEST,³ YOUSAF M. BUTT,³
DIEGO F. TORRES,⁴ AND JOSEP MARTÍ⁵

Received 2007 January 17; accepted 2007 June 6; published 2007 July 11

ABSTRACT

We present a 50 ks observation of the gamma-ray binary LS I +61 303 carried out with the ACIS-I array aboard the *Chandra X-Ray Observatory*. This is the highest resolution X-ray observation of the source conducted so far. Possible evidence of an extended structure at a distance between 5" and 12" toward the north of LS I +61 303 has been found at a significance level of 3.2 σ . The asymmetry of the extended emission excludes an interpretation in the context of a dust-scattered halo, suggesting an intrinsic nature. On the other hand, while the obtained source flux of $F_{0.3-10\text{ keV}} = 7.1^{+1.8}_{-1.4} \times 10^{-12}$ ergs cm⁻² s⁻¹ and hydrogen column density $N_{\text{H}} = (0.70 \pm 0.06) \times 10^{22}$ cm⁻² are compatible with previous results, the photon index $\Gamma = 1.25 \pm 0.09$ is the hardest ever found. In light of these new results, we briefly discuss the physics behind the X-ray emission, the location of the emitter, and the possible origin of the extended emission ~ 0.1 pc away from LS I +61 303.

Subject headings: stars: emission-line, Be — stars: individual (LS I +61 303) — X-rays: binaries — X-rays: general — X-rays: individual (LS I +61 303) — X-rays: ISM

1. INTRODUCTION

LS I +61 303 is a high-mass X-ray binary associated with the galactic plane variable radio source GT 0236+610 (Gregory & Taylor 1978), which shows periodic nonthermal outbursts, on average, every $P_{\text{orb}} = 26.4960 \pm 0.0028$ days (Taylor & Gregory 1982; Gregory 2002). Optical spectroscopic observations show that the system is composed of a rapidly rotating early-type B0 Ve star with a stable equatorial decretion disk and mass loss, and a compact object with a mass between 1 and 4 M_{\odot} orbiting it every ~ 26.5 days (Hutchings & Crampton 1981; Casares et al. 2005; Grundstrom et al. 2007). Spectral line radio observations give a distance of 2.0 ± 0.2 kpc (Frail & Hjellming 1991). Massi et al. (2001, 2004) reported the discovery of an extended jetlike and apparently precessing radio emitting structure at angular extensions of 10–50 mas. Due to the presence of (apparently relativistic) radio emitting jets, LS I +61 303 was proposed to be a microquasar. However, recent VLBA images obtained during a full orbital cycle show a rotating elongated morphology (Dhawan et al. 2006), which may be consistent with a model based on the interaction between the relativistic wind of a nonaccreting pulsar and the wind of the stellar companion (Dubus 2006). The MAGIC Cerenkov telescope has recently detected LS I +61 303 at very high energy gamma rays (≥ 100 GeV; Albert et al. 2006). LS I +61 303 and LS 5039 (Paredes et al. 2000; Aharonian et al. 2005) share the quality of being the only two known X-ray binaries that are also GeV emitters. Therefore, they can be called gamma-ray binaries.

LS I +61 303 has been observed with different X-ray satellites: *Einstein* (Bignami et al. 1981), *ROSAT* (Goldoni &

Mereghetti 1995; Taylor et al. 1996), *ASCA* (Leahy et al. 1997), *RXTE* (Harrison et al. 2000), *BeppoSAX*, *XMM-Newton*, and *INTEGRAL* (Sidoli et al. 2006; Chernyakova et al. 2006). The spectrum could always be fitted with an absorbed power law with values in the ranges $N_{\text{H}} = (0.45-0.65) \times 10^{22}$ cm⁻² and $\Gamma = 1.5-1.9$. The 2–10 keV X-ray flux shows orbital variability (Paredes et al. 1997), with values ranging from ~ 5 to 20×10^{-12} ergs cm⁻² s⁻¹, the maximum occurring at orbital phase ~ 0.5 (assuming $T_0 = \text{JD } 2,443,366.775$). No spectral lines nor extended X-ray emission have ever been reported. Here we present, for the first time, *Chandra* X-ray observations of LS I +61 303, aimed at detecting small-scale extended X-ray emission.

2. CHANDRA OBSERVATIONS AND RESULTS

We observed LS I +61 303 with *Chandra* using the standard ACIS-I setup in VF mode and 3.24 s time frame during a total of 49.9 ks from 2006 April 7 22:30 UT to April 8 12:22 UT (MJD 53,832.9375–53,833.5153). This corresponds to orbital phases 0.028–0.050, when a relatively low flux is expected, thus minimizing possible pileup effects.

The *Chandra* Interactive Analysis of Observations software package (CIAO ver. 3.3.0.1) and the CALDB version 3.2.2 have been used to perform the reduction of level 1 event files, as well as the spectrum and light curve subtraction. The reprocessed level 2 event files have been created to account for readout effects. The position angle of the readout direction of the ACIS-I chip was -62° (positive from north to east).

We have reduced the data using standard procedures given in the *Chandra* analysis threads. The source region has been defined as a 20 pixel ($\sim 10''$) radius circle around the source center. For the background, we took a nearby circular region of 80 pixel ($\sim 40''$) radius, away from the source and the CCD junction. To avoid the presence of possible (very faint) sources in the background, the tool `celldetect` was applied. The `mkacisrmf` and `mkarf` tools were used to generate the RMF and ARF files, respectively. The tool `dmextract` was used to generate the source and the background light curves and spectra. The spectrum was grouped with the tool `dmgroup` to 30 counts per energy bin.

LS I +61 303 showed a moderate level of activity, with

¹ Departament d'Astronomia i Meteorologia, Facultat de Física, Universitat de Barcelona, E-08028 Barcelona, Spain; jmparedes@ub.edu, mribo@am.ub.es.

² Max-Planck-Institut für Kernphysik, D-69117 Heidelberg, Germany; vbosch@mpi-hd.mpg.de.

³ Harvard-Smithsonian Center for Astrophysics, Cambridge, MA 02138; jennifer@head.cfa.harvard.edu, ybutt@head.cfa.harvard.edu.

⁴ Institució Catalana de Recerca i Estudis Avançats (ICREA) and Institut de Ciències de l'Espai (IEEC-CSIC) Campus UAB, Fac. de Ciències, Torre C5, parell, 2a planta, E-08193 Barcelona, Spain; dtorres@aliga.ieec.uab.es.

⁵ Departamento de Física, Escuela Politécnica Superior, Universidad de Jaén, Las Lagunillas s/n, Edificio A3, 23071 Jaén, Spain; jmarti@ujaen.es.

an average count rate of $0.15 \text{ counts s}^{-1}$ (see Fig. 1), and the data were affected by pileup at the $\sim 14\%$ level (see below). The background was very low and estimated to be about 1% of the source count rate within the source region. The position of the X-ray source, determined by using the CIAO package tool `celldetect`, is $\alpha = 02^{\text{h}}40^{\text{m}}31.63^{\text{s}} \pm 0.02^{\text{s}}$, $\delta = 61^{\circ}13'45.70'' \pm 0.3''$ (J2000.0). The errors, as in the rest of this work, are 1σ . The X-ray position is consistent with the radio and optical positions.

2.1. Light Curve

The background-subtracted light curve of LS I +61 303 in the 0.3–10 keV band is plotted at the bottom of Figure 1. Each point represents 324 s of data, and the error bars represent the square root of the total number of counts in each bin divided by 324 s. We have also computed the hardness ratio (HR) by dividing the count rate in the 1.7–10 keV energy range by the corresponding one in the 0.3–1.7 keV range. We show at the top of Figure 1 the HR as a function of time, but with a larger bin time of 1024 s to have relatively small error bars. The count rate is moderately variable on timescales from several minutes to hours, with an average of $0.144 \pm 0.029 \text{ counts s}^{-1}$ ($\chi_{\text{red}}^2 = 1.84$). The count rate increases during the observation, and a linear fit yields a 30% increase at the end with respect to the beginning. Superimposed on this trend is a miniflare 32 ks after the start of the observation, when the count rate increases by a factor of ~ 2 over a timescale of ~ 1000 s, with a total duration of ~ 3 ks. This miniflare is accompanied by an increase of the HR. This kind of moderate variability was first observed with *ASCA*, which detected source variations of about 50% on timescales of half an hour (Harrison et al. 2000). Archival *BeppoSAX* observations carried out in 1997 have also shown short-term variability (Sidoli et al. 2006). It is interesting to note that small-amplitude ($<10\%$) radio flares were detected in LS I +61 303 with a recurrence period of ~ 5 ks (Peracaula et al. 1997). The presence of hour timescale X-ray miniflares has also been reported in the case of LS 5039 (Bosch-Ramon et al. 2005). A hardness versus intensity diagram for the whole *Chandra* observation of LS I +61 303 reveals a positive trend—the source is harder when it is brighter, but with a low significant correlation coefficient of $r = 0.44$. This is in contrast to the clear correlation found in previous *XMM-Newton* observations by Sidoli et al. (2006).

2.2. X-Ray Spectrum

Since the HR is not significantly variable ($\chi_{\text{red}}^2 = 1.78$), we considered the whole data set for the spectral analysis. To perform the spectral fits we restricted the energy range between 0.3 and 10 keV. A fit to the data with a bremsstrahlung model provided $\chi_{\text{red}}^2 = 1.6$, and no lines nor a multicolor blackbody were required to fit the data. An absorbed power-law fit yielded $\chi_{\text{red}}^2 = 1.14$, but a significant excess above 7 keV was apparent in the residuals. Due to the count rate and time frame used, this is probably due to pileup. The addition of the pileup model implemented in *Sherpa* (Davis 2001) to the absorbed power law yielded different sets of possible spectral parameter values, all of them equally compatible from a statistical point of view. Nevertheless, for some of them the derived fluxes were a factor ≥ 5 higher than previous measurements at similar orbital phases. We found that reasonable results were obtained when fixing the event pileup fraction parameter f to 0.95: $\chi_{\text{red}}^2 = 0.83$, grade migration parameter $\alpha = 0.33 \pm 0.09$, $N_{\text{H}} = (0.70 \pm 0.06) \times 10^{22} \text{ cm}^{-2}$, $\Gamma = 1.25 \pm 0.09$, pileup fraction 14%, and $F_{0.3-10 \text{ keV}} = 7.1_{-1.4}^{+1.8} \times 10^{-12} \text{ ergs cm}^{-2} \text{ s}^{-1}$. The significance of adding a pileup component to the absorbed power-

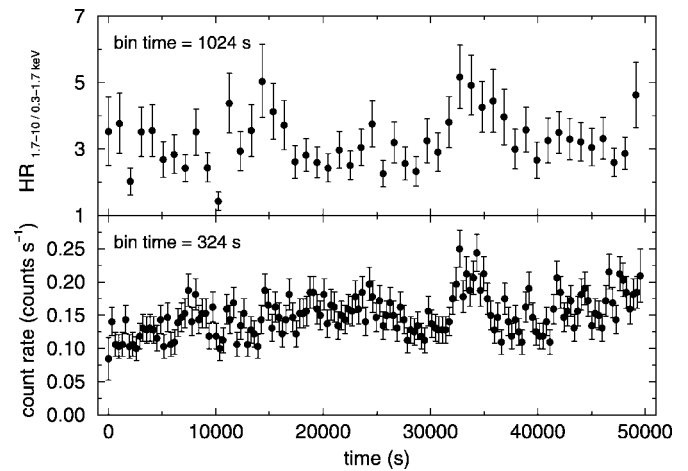


FIG. 1.—*Bottom*: Background-subtracted light curve of LS I +61 303 obtained with *Chandra*. The binning time is 324 s, and the error bars are at the 1σ level. Time origin corresponds to 2006 April 7 at 22:33:17 UT (MJD 53,832.9398), and the observation length is 50 ks. Total count rate variations of a factor of 2 on timescales of a few hours are clearly seen. *Top*: Hardness ratio (HR) between 1.7–10 and 0.3–1.7 keV energy ranges. The binning time has been increased to 1024 s to reduce the size of the error bars. The HR is not significantly variable, and it is poorly correlated with the count rate (except during the miniflare).

law fit was estimated via an F -test: the probability that this improvement happens by chance is 0.8%.

To check the robustness of the results obtained with the spectral fitting with the pileup model we have conducted two additional tests. First of all, we have obtained the spectrum of the readout streak, which is not affected by pileup, after excluding the 5 pixel diameter region around the source. Since it only contains 287 counts, we have fitted the spectrum using low count number statistical weights. Fixing N_{H} to $0.7 \times 10^{22} \text{ cm}^{-2}$, we have obtained $\Gamma = 1.21 \pm 0.14$, which is consistent within errors to the value given above. An additional test has been conducted by fitting the spectrum of the source wings, which are not affected by pileup. We have built a spectrum with data beyond a radius of $1.5''$ from the source center (i.e., excluding the inner 3×3 pixels, those most affected by pileup) and fitted it with and without fixing N_{H} , obtaining in both cases a photon index harder than the one obtained with the pileup model. A similar test with data beyond $2.0''$ has provided similar results. These tests clearly suggest that the photon index value obtained with the pileup model is reliable, and that the source was intrinsically hard during this observation. Moreover, the estimate of the total source flux using the fitted flux of the source wings and the fraction of the simulated PSF (see § 2.3) counts contained in the wings is compatible for $f = 0.95$. This is not the case for the lower values of f that implied the much higher source fluxes discussed in the previous paragraph. These results give us confidence in the results obtained with the pileup model.

Regarding the emission of LS I +61 303 itself, the flux we report here, $F_{0.3-10 \text{ keV}} = 7.1_{-1.4}^{+1.8} \times 10^{-12} \text{ ergs cm}^{-2} \text{ s}^{-1}$, is compatible within errors to that obtained during a short *XMM-Newton* observation also around phase 0 (Chernyakova et al. 2006). However, the photon index $\Gamma = 1.25 \pm 0.09$ found in the *Chandra* data is the hardest ever found, only compatible with any previous value at the 3σ level and harder, at a $\sim 5 \sigma$ level, than the *XMM-Newton* one at the same phase ($\Gamma = 1.78 \pm 0.04$). It is outside the scope of this work to put forward a physical model for the spectral state of the source. We will just point out that the X-ray photon index can be harder than

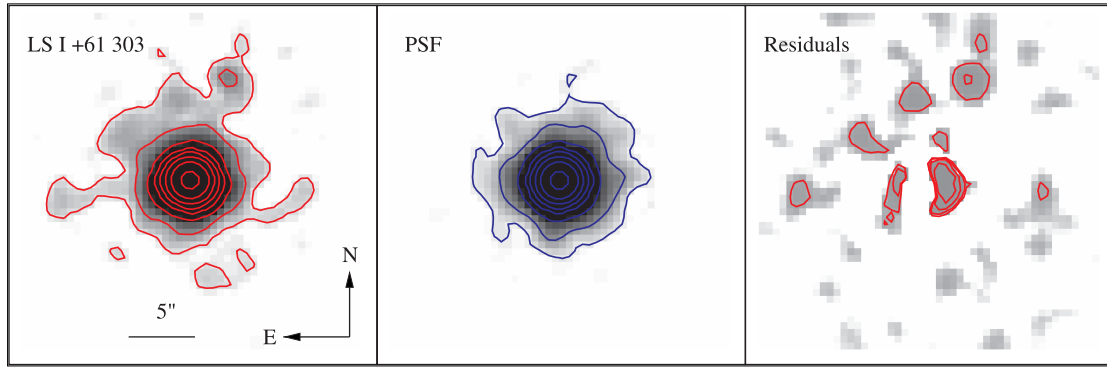


FIG. 2.—*Left*: Image of LS I +61 303 obtained with *Chandra* in the 0.3–10 keV energy range. The image size is $24.5'' \times 24.5''$ (the pixel size is $0.49'' \times 0.49''$). A Gaussian kernel of 3 pixels in radius has been used to smooth the image. The intensity scales logarithmically. The contours correspond to seven logarithmic steps in the range 0.2–300 counts pixel^{-1} . Extended X-ray emission is probably present at a distance of $5''$ – $12''$ from the center. *Middle*: Same as before, but for the PSF. *Right*: Same as before, but for the residuals obtained after subtracting the PSF image to the source one. The intensity scales here via a histogram equalization. The extended emission at distances beyond $5''$, in the form of several spots toward the northeast, is apparent. The central residuals at $\sim 2''$ radius occur within the core of the PSF, and no conclusion can be drawn because of pileup.

the canonical value of 1.5, which corresponds to an electron population with power-law index of 2. This can occur for different reasons, for example, a Klein-Nishina dominated steady particle population (see Derishev 2007 for an extended discussion). A very hard spectral component (e.g., inverse Compton or bremsstrahlung), produced by the lower energy part of the particle spectrum with a high low-energy cutoff, may also harden the synchrotron spectrum. The lack of simultaneous data at higher energies does not allow us to distinguish between the two hypotheses.

We finally selected the data corresponding to the miniflare and obtained a spectrum for it, which had poor statistics and was especially affected by pileup. A fit to this spectrum yielded a photon index compatible within (large) errors to that of the whole observation spectrum.

2.3. Imaging

A preliminary visual inspection of the source image reveals the possible existence of extended emission. To better study this issue we have used ChaRT and MARX to simulate the point-spread function (PSF) accounting for pileup effects. This PSF has the same counts as the source, which are distributed in energy according to the source spectrum including pileup, being spatially

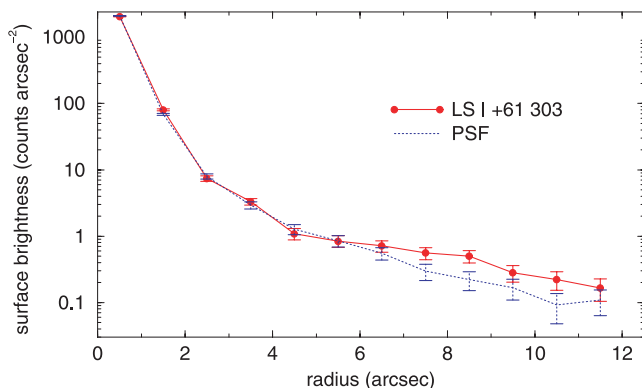


FIG. 3.—Surface brightness distribution of LS I +61 303 (red filled circles) compared to the PSF (dashed blue line). The excess above $\sim 5''$ is apparent in this radial profile, even if the extended emission is asymmetric.

distributed in the image considering pileup as well.⁶ We show in Figure 2 the images corresponding to the source, the PSF, and the residuals obtained after subtracting the PSF from the source, all of them smoothed with a Gaussian kernel of 3 pixels in radius to enhance the faint emission. As can be seen in the left panel of Figure 2, there appears to be extended X-ray emission around LS I +61 303 at distances between $5''$ and $12''$ from the source center. The subtraction of the nearly circular PSF, shown in the middle panel of Figure 2, from the source image yields the residuals shown in the right panel of Figure 2. There seems to be a region with an excess of counts at several arcseconds from the image core and nearly half-surrounding it. This excess region, already apparent in the source image, presents some spots and extends mainly toward the northeast.

To check the reliability of the $5''$ – $12''$ excess we have created radial profiles of the surface brightness for the source and the simulated PSF with the tools `dmextract` and `dmtcalc`. We show the radial profiles with bins of $1''$ in Figure 3, where hints of excess are seen in the region $5''$ – $12''$ away from the center. Moreover, we note that a comparison with the unscattered pointlike blazar source PKS 2155–304 located at high galactic latitude (following the procedure described in Gallo & Fender 2002) provided an even clearer departure of LS I +61 303 from a pointlike source. Nevertheless, we prefer to show here the most conservative results obtained with the PSF, simulated at the chip position and with the observed spectrum of LS I +61 303 including pileup effects. Next we computed the excess of source counts over the PSF in an annulus with inner and outer radii of $5''$ and $12.5''$ and obtained 58 ± 18 counts (3.2σ , or single trial probability of 1.4×10^{-3}). We have looked for excesses in a circle with radius $20''$ centered on the source, without considering the central $5''$ radius circle, thus yielding an area of $\pi(20^2 - 5^2)''^2$. Dividing this by the area of the annulus where we obtained the 3.2σ excess, we find that the number of trials is 2.9, yielding a probability of 4.1×10^{-3} , which corresponds to 2.9σ . However, since the extended emission appears to be asymmetric, we have computed the excess dividing the $5''$ – $12.5''$ annulus in four quadrants. Although there is no excess toward the west and south directions, the excess is of $\sim 1.5 \sigma$ to the east and reaches 3.8σ to the north (or single trial probability of 1.4×10^{-4}). We note

⁶ We note that, while the pileup model included in MARX is valid for qualitative predictions of the effects of pileup on the PSF, it has not been verified for image reconstruction (MARX 4.0 Technical Manual, § 7.3).

that this excess is not located in the path of the readout streak. The number of trials is now 11.6, providing a posttrial probability of 1.6×10^{-3} or a 3.2σ detection. The excess in the northern quadrant of the $5''$ – $12.5''$ annulus, with a projected distance of 0.05 – 0.12 pc from the center of LS I +61 303, represents 0.5% of the source counts, implying (with $\Gamma = 1.25$) a flux of $\sim 4 \times 10^{-14}$ ergs cm^{-2} s^{-1} and $L_x \sim 2 \times 10^{31}$ ergs s^{-1} .

3. DISCUSSION

The *Chandra* observations reported here show that LS I +61 303 presented moderate fluxes of $F_{0.3-10 \text{ keV}} = 7.1_{-1.4}^{+1.8} \times 10^{-12}$ ergs cm^{-2} s^{-1} , as expected around orbital phase ~ 0 (Sidoli et al. 2006). The source appeared to be moderately variable on timescales of ~ 1000 s. The hydrogen column density was $N_{\text{H}} = (0.70 \pm 0.06) \times 10^{22}$ cm^{-2} , similar to the values found in the past. The photon index was 1.25 ± 0.09 , harder than the previously measured values in the range 1.5 – 1.9 . Finally, an excess between $5''$ and $12.5''$ toward the north of LS I +61 303 has been detected at the 3.2σ level (posttrial).

Chandra observations of X-ray binaries have provided the most detailed X-ray images of these sources. Extended circular emission, produced by ISM dust grains along the line of sight that scatter mainly the soft X-rays (Predehl & Schmitt 1995), has been found in most cases (Xiang et al. 2005). However, the possible extended structure around LS I +61 303 we report here is asymmetric, suggesting its intrinsic nature. Plausible explanations of this diffuse radiation could be thermal bremsstrahlung produced by hot and dense ISM close to the source, perhaps heated and compressed by a large-scale outflow originated in LS I +61 303, and synchrotron or inverse Compton emission produced by nonthermal particles accelerated at the termination region of the aforementioned outflow. The first possibility would require a medium with densities significantly higher than those inferred from the ISM absorption toward LS I +61 303. If nonthermal, the extended emission would more likely be of synchrotron origin due to its shorter timescales to radiate at a few keV than those of inverse Compton or relativistic bremsstrahlung.

In any case, the asymmetric distribution of counts could be related to the main direction of the outflow and/or to ISM inhomogeneities. Regardless of the morphology, we can say that efficient energy transport is probably taking place up to distances of at least ~ 0.1 pc in LS I +61 303. However, only deeper high-resolution observations can help to better detect the excess (currently at a 3.8σ level, 3.2σ posttrial) and determine the precise morphology and underlying physics.

A final comment on the hydrogen column density appears necessary. The N_{H} value inferred from spectral fits to all available X-ray observations is in the range $(0.45$ – $0.70) \times 10^{22}$ cm^{-2} , while the N_{H} value of the ISM inferred from UV/optical absorption is in the range $(0.45$ – $0.60) \times 10^{22}$ cm^{-2} . Therefore, the detected X-rays suffer small intrinsic absorption, if any. Moreover, no significant N_{H} orbital variations have ever been detected (as pointed out previously by Leahy et al. [1997] after ASCA observations). In conclusion, the apparent lack of significant soft X-ray absorption and the constancy of N_{H} along the orbit are difficult to be explained, considering the slow and dense material expelled from the companion star. The X-ray emitter should be placed away from the binary system to produce such observational results, in contrast with the expectations from classical colliding wind and microquasar scenarios. This issue certainly requires further investigation.

We thank Mike Nowak for helpful discussions on the analysis of the *Chandra* data. J. M. P., M. R., V. B.-R. and J. M. acknowledge support by DGI of the Spanish Ministerio de Educación y Ciencia (MEC) under grants AYA2004-07171-C02-01 and AYA2004-07171-C02-02 and FEDER funds. M. R. acknowledges financial support from MEC through a *Juan de la Cierva* fellowship. V. B.-R. thanks the Max-Planck-Institut für Kernphysik for its support and kind hospitality. J. R. W. was supported by Cycle 7 *Chandra* grant GO6-7025X. D. F. T. has been supported by MEC under grant AYA-2006-00530, and the Guggenheim Foundation. J. M. is also supported by PAI of Junta de Andalucía as research group FQM322.

Facility: CXO

REFERENCES

- Aharonian, F., et al. 2005, *Science*, 309, 746
 Albert, J., et al. 2006, *Science*, 312, 1771
 Bignami, G. F., Caraveo, P. A., Lamb, R. C., Markert, T. H., & Paul, J. A. 1981, *ApJ*, 247, L85
 Bosch-Ramon, V., Paredes, J. M., Ribó, M., Miller, J. M., Reig, P., & Martí, J. 2005, *ApJ*, 628, 388
 Casares, J., Ribas, I., Paredes, J. M., Martí, J., & Allende Prieto, C. 2005, *MNRAS*, 360, 1105
 Chernyakova, M., Neronov, A., & Walter, R. 2006, *MNRAS*, 372, 1585
 Davis, J. E. 2001, *ApJ*, 562, 575
 Derishev, E. V. 2007, *Ap&SS*, in press (astro-ph/0611260)
 Dhawan, V., Mioduszewski, A., & Rupen, M. 2006, in Proc. VI Microquasar Workshop: Microquasars and Beyond, ed. T. Belloni (Trieste: PoS), 52
 Dubus, G. 2006, *A&A*, 456, 801
 Frail, D. A., & Hjellming, R. M. 1991, *AJ*, 101, 2126
 Gallo, E., & Fender, R. P. 2002, *MNRAS*, 337, 869
 Goldoni, P., & Mereghetti, S. 1995, *A&A*, 299, 751
 Gregory, P. C. 2002, *ApJ*, 575, 427
 Gregory, P. C., & Taylor, A. R. 1978, *Nature*, 272, 704
 Grundstrom, E. D., et al. 2007, *ApJ*, 656, 437
 Harrison, F. A., Ray, P. S., Leahy, D. A., Waltman, E. B., & Pooley, G. G. 2000, *ApJ*, 528, 454
 Hutchings, J. B., & Crampton, D. 1981, *PASP*, 93, 486
 Leahy, D. A., Harrison, F. A., & Yoshida, A. 1997, *ApJ*, 475, 823
 Massi, M., Ribó, M., Paredes, J. M., Garrington, S. T., Peracaula, M., & Martí, J. 2004, *A&A*, 414, L1
 Massi, M., Ribó, M., Paredes, J. M., Peracaula, M., & Estalella, R. 2001, *A&A*, 376, 217
 Paredes, J. M., Martí, J., Peracaula, M., & Ribó, M. 1997, *A&A*, 320, L25
 Paredes, J. M., Martí, J., Ribó, M., & Massi, M. 2000, *Science*, 288, 2340
 Peracaula, M., Martí, J., & Paredes, J. M. 1997, *A&A*, 328, 283
 Predehl, P., & Schmitt, J. H. M. M. 1995, *A&A*, 293, 889
 Sidoli, L., Pellizzoni, A., Vercellone, S., Moroni, M., Mereghetti, S., & Tavani, M. 2006, *A&A*, 459, 901
 Taylor, A. R., & Gregory, P. C. 1982, *ApJ*, 255, 210
 Taylor, A. R., Young, G., Peracaula, M., Kenny, H. T., & Gregory, P. C. 1996, *A&A*, 305, 817
 Xiang, J., Zhang, S. N., & Yao, Y. 2005, *ApJ*, 628, 769